Petroleum and Coal

Article Open Access

Seismic Attributes Analysis and Petrophysical Evaluation of Reservoir Sand Units in "Mars" Field, Onshore Niger Delta Basin, Nigeria

Okewu Godwin Onah[1], Ugbor Desmond Okechukwu[1], Johnson Ibuot[1], John Akor Yakubu[1], Eze Martins Okoro[2] and Kentsa Tchakam Steven[1]

[1] *Department of Physics and Astronomy, University of Nigeria Nsukka, Nigeria*
[2] *Department of Geology, University of Nigeria Nsukka, Nigeria*

Received April 15, 2024; Accepted August 13, 2024

Abstract

Seismic attribute analysis and petrophysical evaluation of the "Mars" Field onshore Niger Delta Basin was carried out in this study to characterize hydrocarbon-bearing reservoir units in the field. The study utilized 3D seismic and well log data to delineate hydrocarbon zones and reservoir sands of interest, estimate the petrophysical properties of the reservoirs, and map the structural framework of the field to ascertain the lateral variability of the reservoir properties. Data from five wells comprising gamma rays, resistivity, neutrons, density, and sonic logs were used. Gamma-ray logs enabled the discrimination of sand and shale lithologies, while the reservoir porosities were calculated from density logs. The combination of neutron and density logs with resistivity logs aided in the identification of hydrocarbon-saturated zones in the field. Three hydrocarbon-bearing reservoirs were delineated and designated as F_0004, G_0006, and H_0008 reservoir sands. The sands show thickness variations between 9 and 79 m, with porosities ranging from 12% to 27%. The reservoir tops corresponded with the mapped horizons from the seismic data. A total of four structure-building faults were mapped in the field. Seismic attributes extractions over the mapped horizons (sand tops) revealed booming amplitude zones interpreted to represent hydrocarbon leads and potential prospective zones at different stratigraphic intervals in the field. Further studies are required to ascertain the potentiality and producibility of the identified hydrocarbon zones in the study area.

Keywords: *Seismic attributes analysis; Petrophysical evaluation; Reservoir sands; Niger Delta Basin.*

1. Introduction

The Niger Delta Basin is a mature hydrocarbon province with most oilfields already beyond their peak and currently witnessing declining productions. With most exploration activities on hold due to low-price oil market, the need therefore arises to prolong the life span of these mature assets by re-evaluating the existing datasets to discover new prospect opportunities and potential areas for infill drilling and increased production.

Characterizing the hydrocarbon reservoirs in the Niger Delta Basin is a major challenge for explorationists due to subsurface complexities introduced by the presence of faults and heterogeneous nature of the depositional sand-shale facies [1-3]. [4] noted the controls of syn-depositional structures on reservoir heterogeneities in the Niger Delta. The hydrocarbon traps identified in the basin are mainly growth faults and roll-over anticlinal structures, stratigraphic traps, or a combination of both [5]. These traps are formed in different depositional settings which exert a major influence on the quality, producibility and overall performance of the reservoirs [6]. Hence, understanding the variations in reservoir characteristics is critical for increased productivity from already explored areas, and in the identification of potential prospective zones in the Niger Delta region.

Several workers have carried out reservoir studies in the Niger Delta Basin using attributes extracted from seismic and well log data. [7] opined that initial understanding of the reservoir properties, including porosity, permeability, water saturation, thickness, and areal extent, is crucial in determining hydrocarbon potential of any basin because they serve as necessary and important inputs for reservoir volumetric/economic analysis. [8] integrated results obtained from seismic and petrophysical interpretation to characterize the properties of sand reservoirs in Arike Field of the Niger Delta, Nigeria. Their study provided vital information that will enhance future development of the identified hydrocarbon targets in the field. [9] employed seismic attribute analysis to study reservoir characteristics and identify hydrocarbon prospective zones in the Zech Field, Onshore Niger Delta Basin, Nigeria. Their study revealed amplitude supported hydrocarbon zones, and also showed that data integration and analytical techniques is critical to unravel potential prospective areas in the subsurface that are characterized by high quality reservoir sand units. [4] integrated modern 3D seismic, composite well log data, and petrophysical analysis in the prospectivity evaluation of hydrocarbon reservoir sands in Fega Field located in the onshore Niger Delta Basin, Nigeria. Their study demonstrated the important use of reprocessed 3D seismic data to update reservoir information, which may open up new opportunities by increasing the chances of winning new oil in already explored areas.

The present study utilizes 3D seismic and well log data to investigate the hydrocarbon potentials of the Mars Field, onshore Niger Delta Basin. The integration of seismic attributes analysis and petrophysical evaluation will improve our understanding of the subsurface variabilities in reservoir properties and hydrocarbon prospectivity in the study area.

2. Geologic setting

The "Mars" Field is located in the eastern portion of the Central Swamp Depobelt, onshore Niger Delta Basin (Fig. 1).

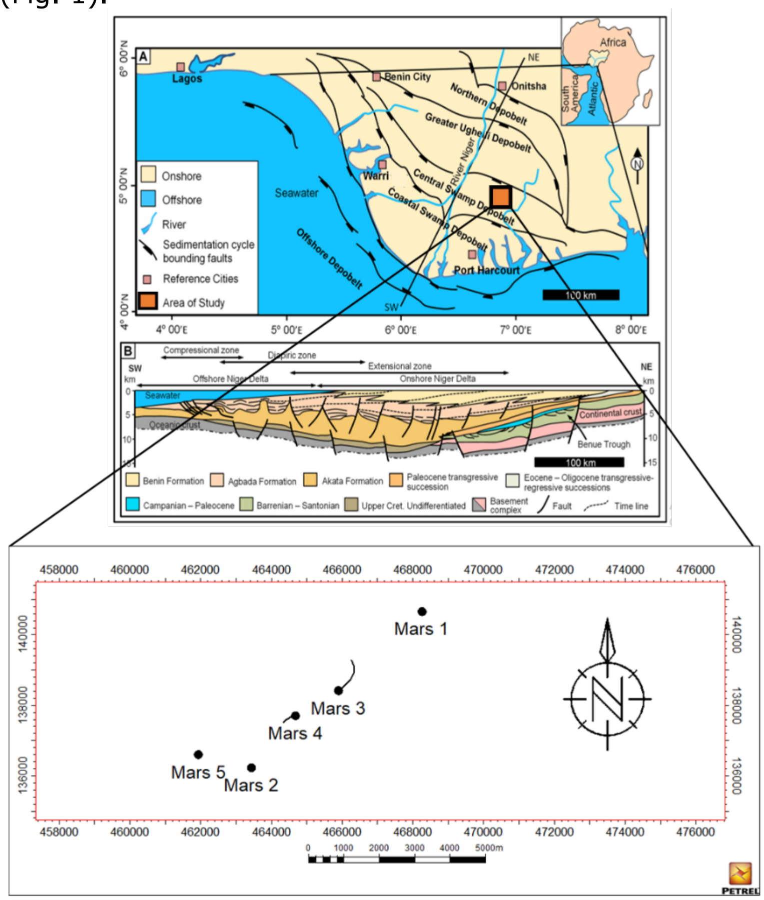

Fig. 1. Regional geological setting of the Niger Delta Basin showing (A) the depobelts and the study area (brown box). (B) Schematic stratigraphic cross-section of the Niger Delta Basin showing the various structural zones (modified from [4]).

The Niger Delta Basin lies within the Gulf of Guinea of West Africa, covering a total area of about 300,000 square kilometers. The infill of the basin comprises mostly of Paleocene to Recent siliciclastic sediments deposited in a fluvial-dominated deltaic setting ranging from shoreface to beach ridges, tidal channels, mangrove swamps, freshwater swamps, and off-shore depositional systems [5,10]. The tectonic evolution of the Niger Delta Basin has been associated with the Early Cretaceous rifting phase that opened up the South Atlantic as the South American and the African Plates separated from each. The rifting which occurred at the site of a triple junction, started in the Late Jurassic and culminated in the Early Cretaceous times [11–13]. Deltaic deposition in the basin started from Eocene, and continued to the Recent time, prograding from north to south, with well-developed depocenters (depobelts) defined by regional and counter-regional growth fault structures [5,14].

The lithostratigraphic units in the Niger Delta Basin (Fig. 2) include the Palaeocene - Miocene Akata Formation, composed mainly of overpressured marine shales. This formation is overlain by the Eocene - Recent Agbada Formation which comprises interbedded fluvio-deltaic sandstone and shales. The Agbada Formation underlies the Oligocene - Recent Benin Formation, mainly made up of continental coastal plain sands and gravels [1, 5,15].

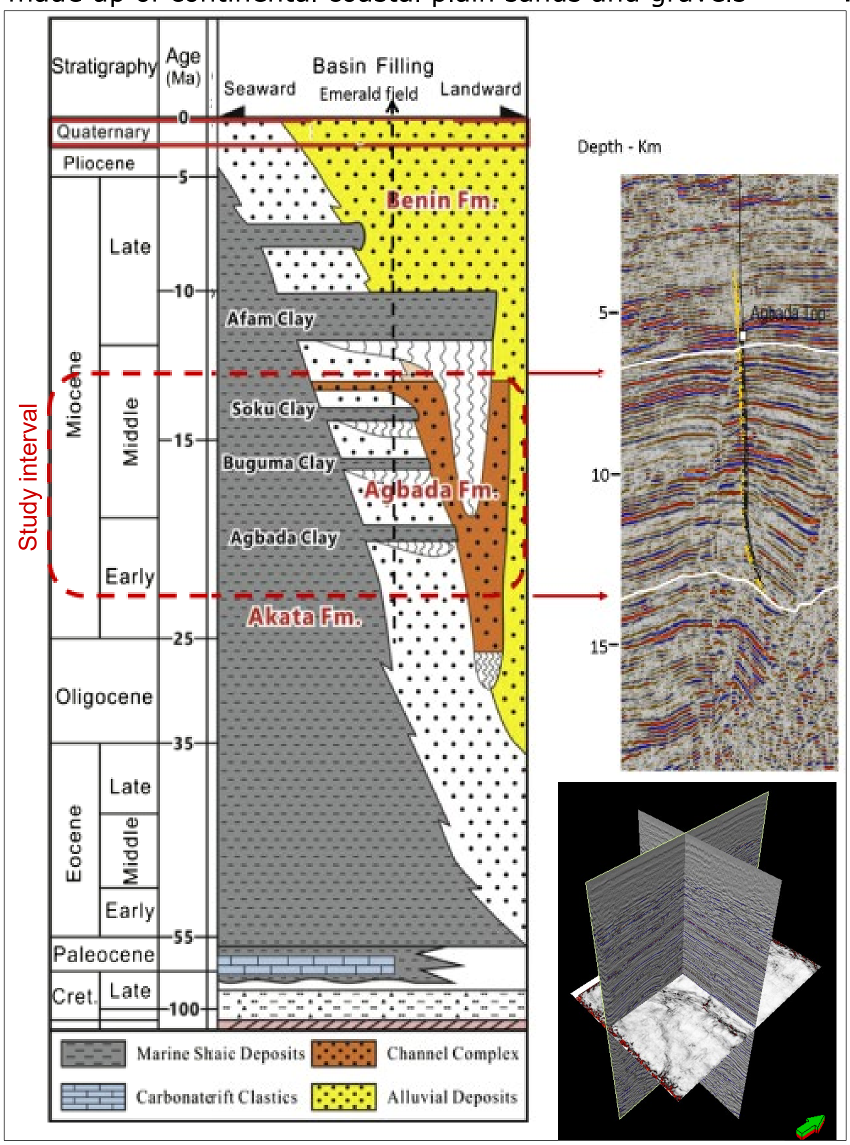

Fig. 2. Niger Delta regional stratigraphic column showing the three main lithostratigraphic units (modified after [5]).

3. Materials and methods

3.1. Materials

The dataset used for this study include 3D seismic volume covering the field, composite log suites from five wells (comprising of gamma rays, resistivity, neutrons, density, and sonic logs), and checkshot data. The name of the field and the wells used in this study were renamed for proprietary reasons to avoid conflict of interest.

3.2. Methods

3.2.1. Well log analysis and petrophysical evaluation

Analysis of the available log suites started by lithologic correlation of the wells using the gamma ray and resistivity log motifs to delineate reservoir (sand) and non-reservoir (shale) intervals. The correlation was carried out along a transect line to understand the reservoir distribution both in the dip (North-South) and strike (East- West) directions across the study area. The neutron and density logs were combined with resistivity logs to identify hydrocarbon-saturated reservoir zones in the field.

Petrophysical evaluation of the delineated reservoir units was carried out to establish hydrocarbon presence in field. This was achieved by the calculation of key reservoir parameters including volume of shale (V_{sh}), total porosity (Ø), net-to-gross ratio (N/G), and water saturation (S_w), using standard petrophysical equations [17]. The empirical equations used in computing the reservoir properties are given below:

Volume of shale (V_{sh}), which defines the percentage of shale contained in a sandstone or heterolithic reservoir, was calculated using the Larionov model for sediments of Tertiary age [16]:

$$V_{sh} = 0.083 * (2^{3.7*I_{GR}} - 1) \quad (1)$$

where I_{GR} is the gamma ray index and is given by:

$$I_{GR} = \frac{(GR_{log} - GR_{min})}{(GR_{max} - GR_{min})} \quad (2)$$

where GR_{log} is the gamma ray reading; GR_{min} is the minimum gamma ray reading (from a clean sandstone formation); and GR_{max} is the maximum gamma ray reading (from a shale or clay formation).

Porosity (Ø), defines the percentage of void spaces to the total rock, was derived from density the log using equation (3) [17]:

$$\emptyset = \frac{(\rho_m - \rho_b)}{(\rho_m - \rho_b)} \quad (3)$$

where Ø is density-derived total porosity; ρ_m is the matrix density; ρ_b is bulk density; and ρ_f is fluid density.

Net-to-Gross (N/G), which is the ratio of the thickness of the clean, porous and permeable, productive (Net) reservoir sand to the total (Gross) reservoir thickness, was determined using the algorithm:

$$N/G = IF(V_{sh} \leq 0.40, (1 - V_{sh}), 0) \quad (4)$$

It is usually not constant across a reservoir and may change over a short lateral distance from 1 (clean reservoir) to 0 (non-reservoir).

Water saturation (S_w) was calculated using the Archie's equation given as:

$$S_w = \left(\frac{FR_w}{R_t}\right)^{\frac{1}{n}} \quad (5)$$

where n is the saturation exponent (usually 2), R_w is the formation water resistivity, R_t is the true rock resistivity (i.e. resistivity of the uninvaded zone), and F is the formation factor, derived using the formula:

$$F = \frac{0.62}{\emptyset^{2.15}} \quad (6)$$

where 0.62 is a constant value for the tortuosity factor and was used in this algorithm for unconsolidated Tertiary rocks of the Niger Delta.

3.2.2. Well - seismic calibration

In order to establish a relationship between the seismic (time domain) and well log (depth domain) data, a synthetic seismogram was generated by convolving the reflectivity and impedance derived from digitized sonic and density logs with the wavelet derived from seismic data. The synthetic seismogram was combined with the available checkshot data to achieve a better tying of the wells to the seismic data. The well-to-seismic tie formed the first step in picking seismic events (horizons), which corresponded to the sand tops of interest, for interpretation.

3.2.3. Seismic interpretation

Interpretation of faults and horizons on the seismic section was carried out along the dip (inline) and strike (crossline) directions to understand the structural framework of field. The faults were identified as reflection discontinuity on the seismic inlines and vertical displacement of reflections. The fault mapping process were aided by the variance edge attribute time slices [18]. Four (4) synthetic faults were mapped and named F1, F2, F3 and F4. The horizons of interest were mapped on the seismic inlines and crosslines based on the amplitude, continuity, and strength of reflections. The picked horizons indicate the gross reservoir units laterally and vertically, and were used to generate time structural maps. The time structural maps were converted to depth structural maps of the reservoir tops using a velocity model generated by applying a polynomial function derived from the checkshot data.

3.2.4. Seismic attributes analysis

Seismic attributes including Root Mean Square (RMS) amplitude and Average Envelope were extracted from the generated maps [18]. The attributes enhance the delineation of geological features and fluid presence in the subsurface. High amplitude zones aided the identification of potential hydrocarbon prospects in the study area.

4. Results and discussion

4.1. Well log correlation and reservoir delineation

Well log panel showing the correlated reservoir sand bodies is presented in Figure 3. Lithological correlation of the logs was used to establish the direction of thickness and lateral continuity of the reservoirs. From the well correlation, it was observed that sediment thickness increases down-dip, synonymous with the overall direction of sediment thickness in the Niger Delta Basin [5].

The identified lithologic units in the studied wells include sand and shale sequences with distinctive log signatures, typical of the alternating sand - shale layers of the Agbada Formation. The composite logs from the studied wells were very useful because they provided a reliable continuous record and detailed information of the different lithologies penetrated by the wells, as well as their spatio-temporal distribution across the field [19]. The log responses were matched for similarity and aided in distinguishing the different subsurface lithologies such as reservoirs (sands) from none reservoirs (shales/clays). The lithologic units were delineated in vertical succession across the field by combining gamma ray and resistivity log responses for the five wells. High gamma ray log signatures correlated to values ranging from 75 API up to 150 API, and were interpreted as shale (or clay) units rich in radioactive materials. Low gamma ray signatures with values ranging between 0 – 75 API were interpreted as sand units with low radioactive material content [20].

Three (3) hydrocarbon-bearing sand reservoirs were delineated in the field (Fig. 3). These sand reservoir units (yellow), designated as F_0004, G_0006 and H_0008, were identified based on the combination and interpretation of gamma ray, resistivity, density and neutron porosity logs. These reservoirs were further analyzed to determine the variations in their petrophysical properties. The correlation was used to understand the lateral distribution, continuity and geometry of reservoirs across the field.

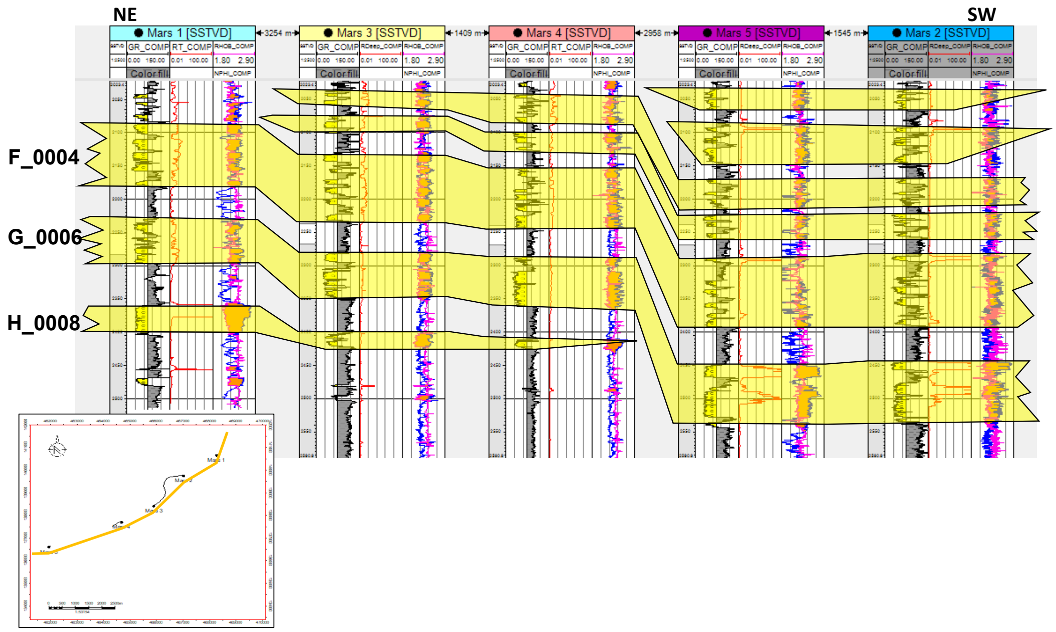

Fig. 3. Well log panel showing the correlated reservoir sand bodies (yellow). F_0004, G_0006 and H_0008 are the three main reservoir sand units identified in the study area. Inset map of the study area showing the well correlation transect.

4.2. Petrophysical interpretations

The summary of the estimated petrophysical properties of three (3) main reservoir units in the study area are presented in Tables 1-5. The 3 sand units cut across the five wells evaluated in this study, except for H_0008 sand which only appeared in Mars 1, Mars 3 and Mars 4 wells, respectively. The reservoirs have high sand - shale ratio, with a general increase in shale content with depth. F_0004 sand vary in thickness between 66 – 95 m, with net-to-gross (N/G) ratio ranging from 0.56 – 0.76, and porosity (Ø) within the range of 20 – 25 %. The overall water saturation in this reservoir is less than 45 %, suggesting that the sand unit is saturated by over 50% hydrocarbon. G_0006 reservoir sand range in thickness from 44 – 95 m, with porosity ranging between 23 – 27 % and water saturation in the range of 25 – 45 %. H_0008 reservoir sand varies in thickness between 6 – 9 m, with water saturation ranging from 38 – 73 %. The reservoir porosity range between 12 – 21 %, with net-to-gross greater than 33 %.

Table 1. Estimated petrophysical properties from Mars 1 well.

Reservoir	Top(m)	Base (m)	Thickness (m)	Vsh	N/G	Ø	Sw
F_0004	2230	2296	66	0.34	0.66	0.20	0.43
G_0006	2360	2404	44	0.31	0.69	0.26	0.38
H_0008	2469	2480	11	0.57	0.43	0.21	0.38

Table 2. Estimated petrophysical properties from Mars 2 well.

Reservoir	Top(m)	Base (m)	Thickness (m)	Vsh	N/G	Ø	Sw
F_0004	2444	2534	90	0.38	0.62	0.25	0.35
G_0006	2445	254	95	0.27	0.23	0.23	0.25
H_0008	-	-	-	-	-	-	-

Table 3. Estimated petrophysical properties from Mars 3 well.

Reservoir	Top(m)	Base (m)	Thickness (m)	Vsh	N/G	Ø	Sw
F_0004	2281	2349	68	0.44	0.56	0.24	0.39
G_0006	2280	2350	70	0.31	0.69	0.27	0.27
H_0008	2494	2503	9	0.64	0.36	0.12	0.53

Table 4. Estimated petrophysical properties from Mars 4 well.

Reservoir	Top(m)	Base (m)	Thickness (m)	Vsh	N/G	Ø	Sw
F_0004	2287	2360	73	0.33	0.67	0.21	0.44
G_0006	2385	2460	75	0.06	0.94	0.26	0.45
H_0008	2483	2489	6	0.56	0.44	0.15	0.73

Table 5. Estimated petrophysical properties from Mars 5 well.

Reservoir	Top(m)	Base (m)	Thickness (m)	Vsh	N/G	Ø	Sw
F_0004	2449	2554	95	0,24	0,76	0,24	0,37
G_0006	2550	2629	79	0,26	0,74	0,27	0,35
H_0008	-	-	-	-	-	-	-

where Vsh = Volume of shale, N/G = Net to Gross Ratio, Ø = Porosity and S_w = Water saturation.

Hydrocarbon saturation in the reservoirs were established based on the observed high resistivity kick and the development of a “balloon structure” due density - neutron log crossover resulting from the high porous nature of the sands. The presence of hydrocarbon in a sand reservoir result in apparent increase in the density log reading, and the corresponding decrease in the neutron log signature, leading to what is known as the gas effect (or balloon structure), where the two log signals separate from each other. Oil in the reservoir causes increase in density-neutron separation, but this is usually very small compared to that due to the presence of gas in the same reservoir [4]. In water bearing zones, resistivity readings are low and are also characterized by tramlining between density and resistivity logs. Density decreases when the water is replaced by oil in a porous reservoir rock. Thus, hydrocarbon bearing zones are characterized both by high resistivity and anti-correlation between the density and the resistivity log [21]. In general, the petrophysical evaluation of the sands show variabilities in the reservoir properties of the identified hydrocarbon zones in the field.

4.3. Well-to-seismic tie

The well-to-seismic tie at the vicinity of Mars 2 well is presented in Figure 4. The well-to-seismic tie was done to obtain an accurate time-depth relationship between the penetrated sequences in the well and their seismic responses, so that horizons can be picked both in time or depth. The well-to-seismic tie showed a fair to good match between the well logs and seismic data, also aided the mapping of horizons of interest corresponding to the evaluated reservoir sand tops.

4.4. Fault and horizon interpretation

The faults interpreted in the study area are presented in Figure 5. The variance attribute extracted from the seismic volume enhanced the imaging and picking of faults along the dip direction (inline), to understand the structural pattern of the field. The mapped faults are curvilinear in nature, trending dominantly in the E - W direction and dipping to the south, except F3 which trends in the NW – SE direction and dipping to the southwest. The area is characterized by high-angle steeply dipping listric (growth) faults and their corresponding roll-over anticlines which form the main trapping geometry in the Niger Delta Basin. Doust and Omatsola interpreted these faults to be syn-sedimentary deformations that originated from rapid sediment loading and gravity tectonics [5]. Growth faults controlled the deposition of thick sedimentary packages in several depo-axis within the Niger Delta Basin [5,22].

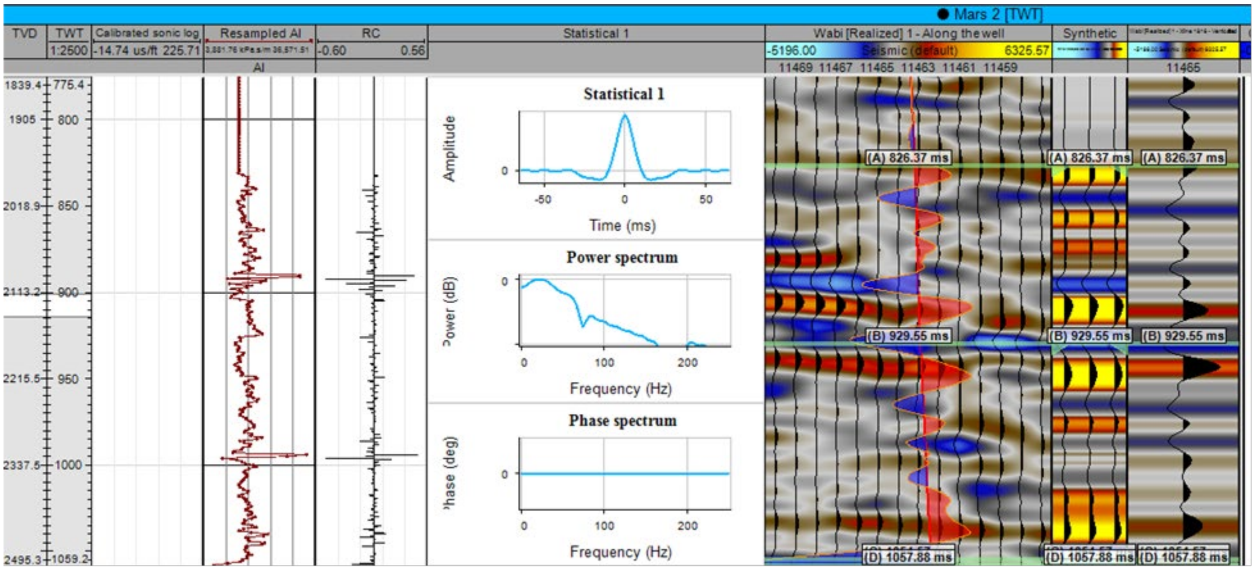

Fig. 4. Well section showing the well-to-seismic tie for Mars 2 well.

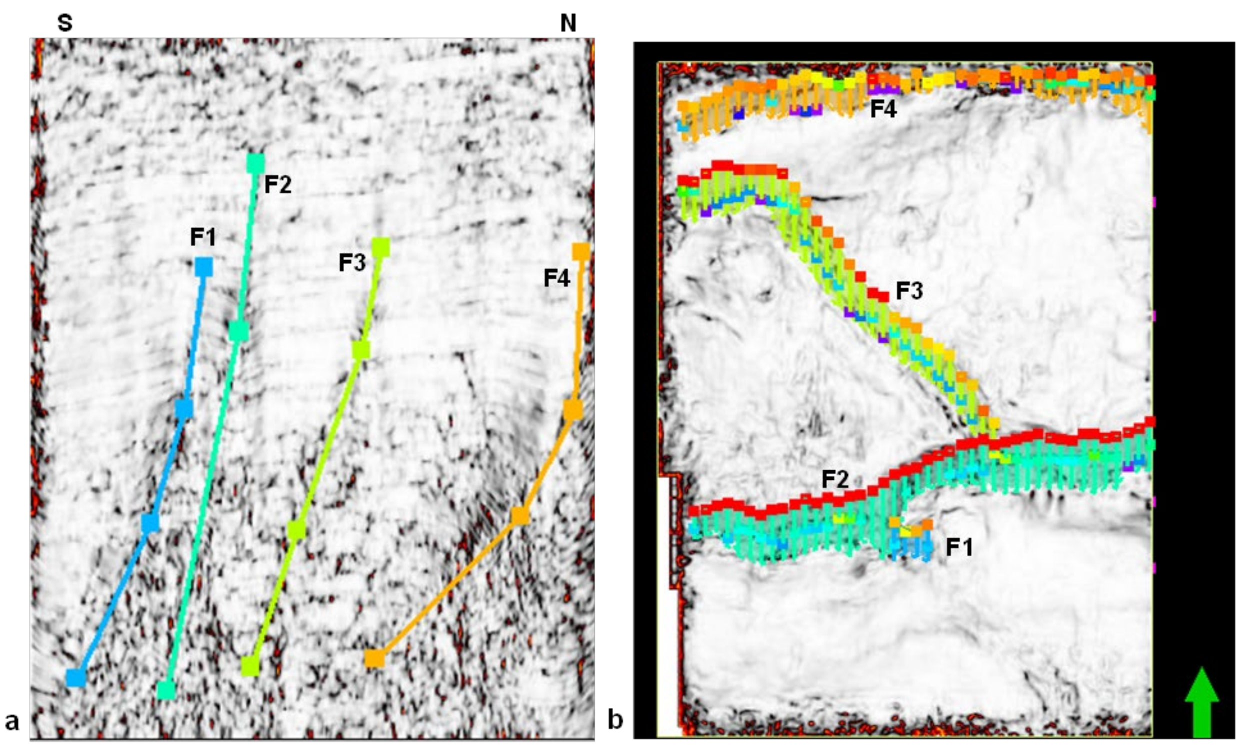

Fig. 5. (a) Seismic variance attributes section showing the mapped faults in the field and (b) variance time slice used to constrain the fault mapping process.

The interpreted horizons (Fig. 6) corresponded to the top of the identified hydrocarbon-bearing reservoir sands from well log analysis. The picked horizons were used to produce the time structural maps (Fig. 7) and depth structural maps (Fig. 8) of the F_0004, G_0006 and H_0008 reservoir sands, respectively. The mapped horizons combined with the interpreted faults to define the structural framework of the study area and variations in the seismic and reservoir properties across the field.

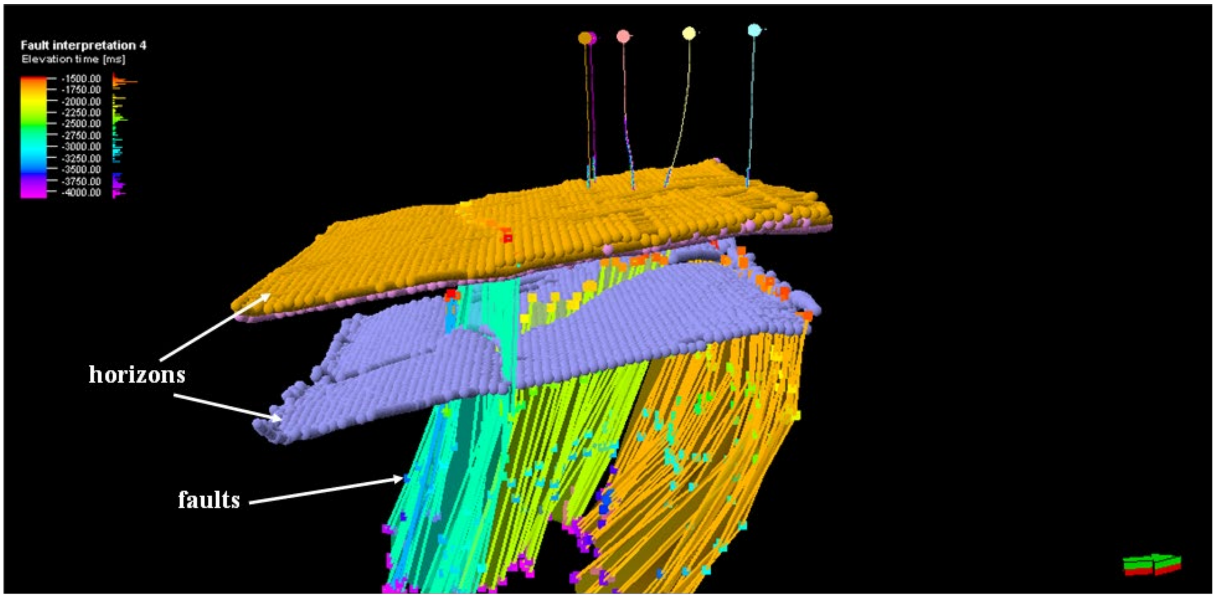

Fig. 6. 3D display of the interpreted horizons and faults.

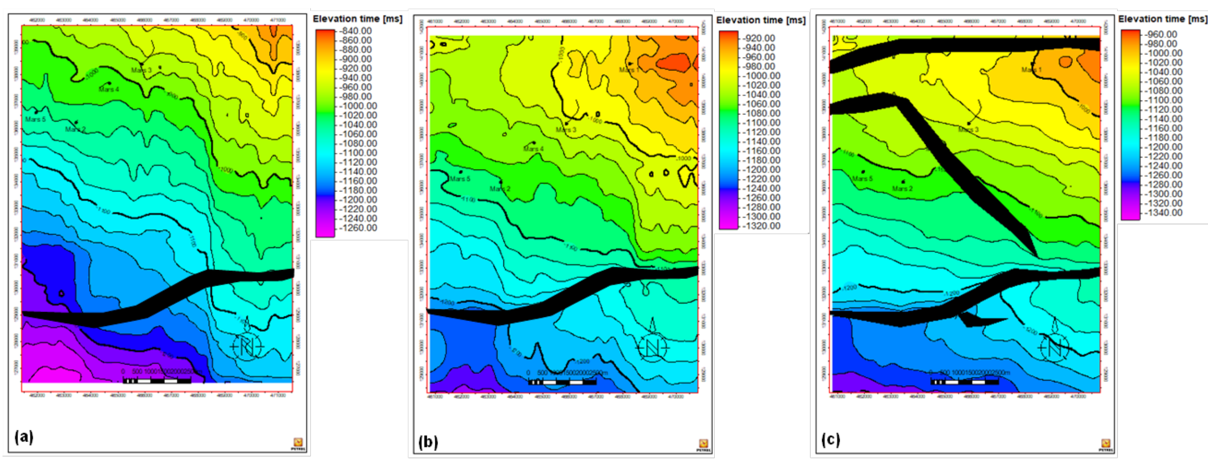

Fig. 7. Time structure map of (a) F_0004 reservoir top, (b) G_0006 reservoir top and (c) H_0008 reservoir top.

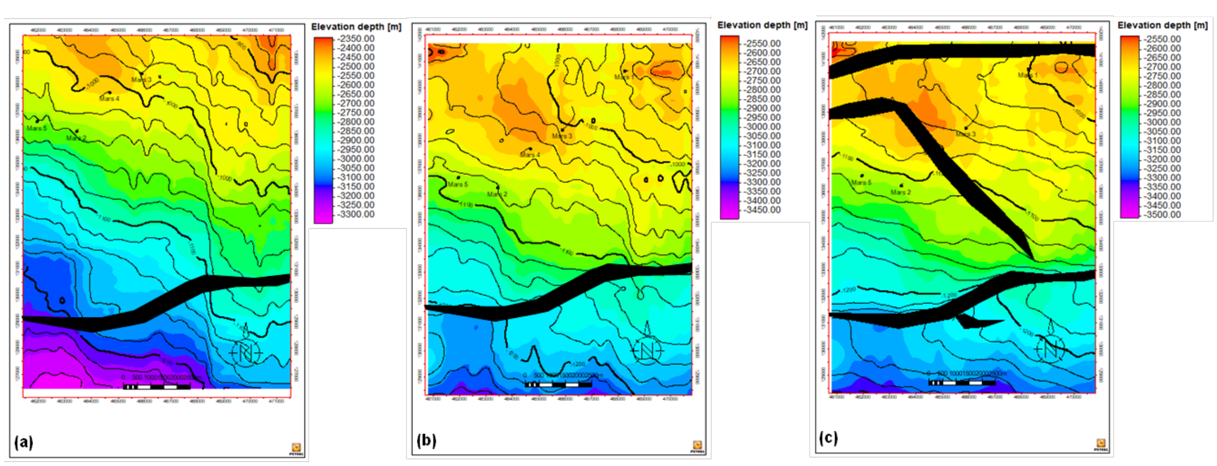

Fig. 8. Depth structure map of (a) F_0004 reservoir top, (b) G_0006 reservoir top and (c) H_0008 reservoir top.

4.5. Structural framework of the field

The structural geometry of the field gave insights on the impacts that both major and minor faults have on subsurface fluid flow and trap styles in the study area. The structures also played a key role in the identification of fault-dependent hydrocarbon leads and prospect prediction from seismic attributes interpretation in this study.

The structural framework of the study area obtained by combining the depth-converted reservoir tops (horizons) and the modeled fault surfaces, shaded light on the overall geometry of the reservoir intervals (Fig. 9). The model was used to define the topographical relationships between the interpreted seismic and well data [23]. The structural style and trapping mechanism of the field is comprised of anticlinal closures and fault-dependent traps. The five wells used in this study, penetrated the shallower F_0004 and G_0006 reservoirs, defined by anticlinal closure, while the deeper H_0008 penetrated by three of the wells (Mars 1, Mars 3 and Mars 4) is defined by fault-dependent closure with key uncertainties ranging from overpressure and possible cross fault leakage of the H_0004 sand reservoir. The structural framework model of the area revealed that the mapped horizons (seismic events and surfaces) are within the hanging wall closure of the faults. The risk associated with such hydrocarbon trap in the area of study include fault shadow effect which may result in poor structural definition and across fault leakage due to poor sealing integrity of the fault. The closures were formed by the intersection of the major east-west trending growth fault and a northwest-southeast trending fault in the Mars field.

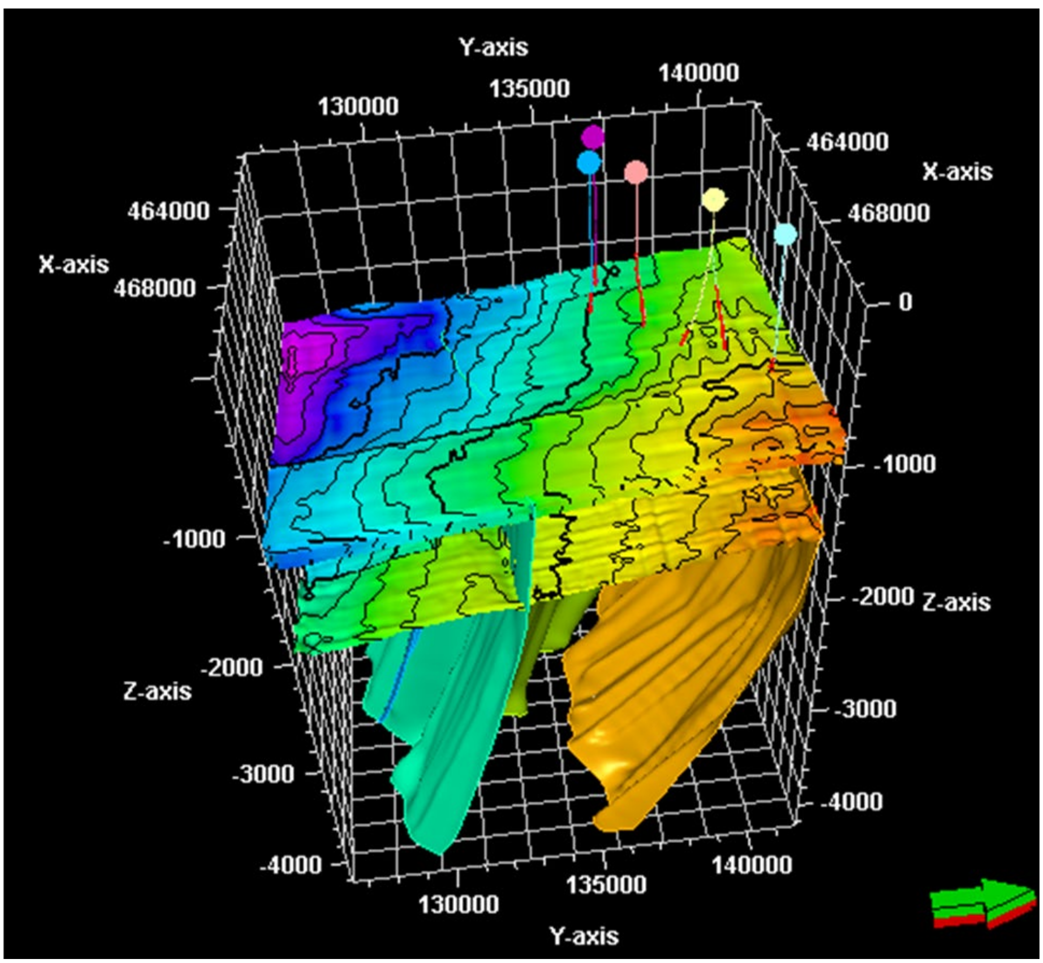

Fig. 9. Structural framework model of the field.

4.6. Seismic attributes interpretation and prospect delineation

Seismic attributes, including RMS amplitude and Average Envelope, extracted from the interpreted horizons (reservoir tops) served as good measure for detecting hydrocarbon presence and identification of new prospective zones in the study area. These attributes revealed anomalous high amplitude zones over the northern part of F_0004 reservoir top (Fig. 10). High amplitude anomalies were also observed in the western portion of G_0006 reservoir top (Fig. 11), as well as in the northeastern, eastern and western portions of H_0008 reservoir top (Fig. 12). The amplitude anomalies conform with the structural configuration of the field.

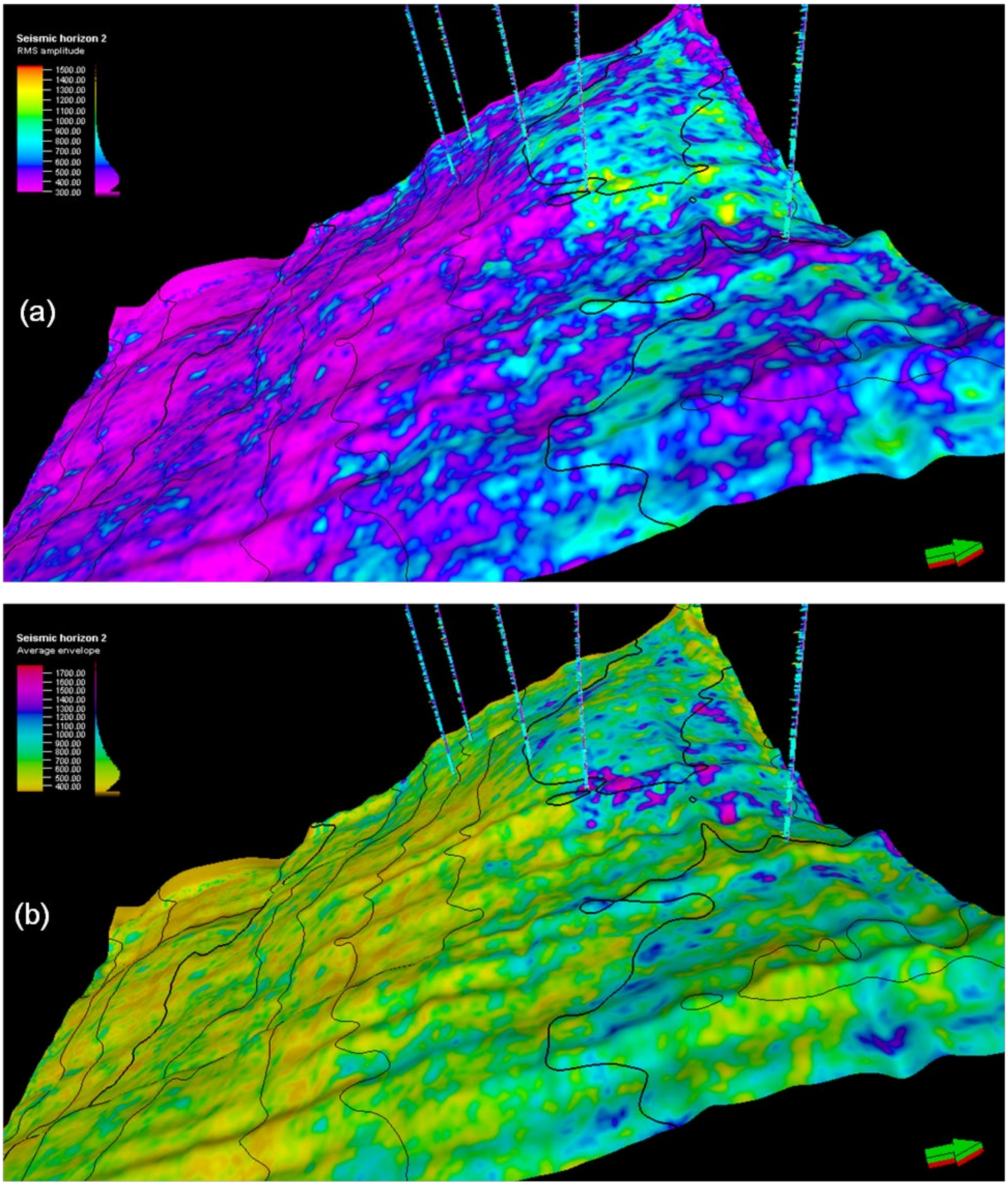

Fig. 10. 3D display of the F_0004 reservoir top with the extracted (a) RMS amplitude, and (b) Average Envelope attributes.

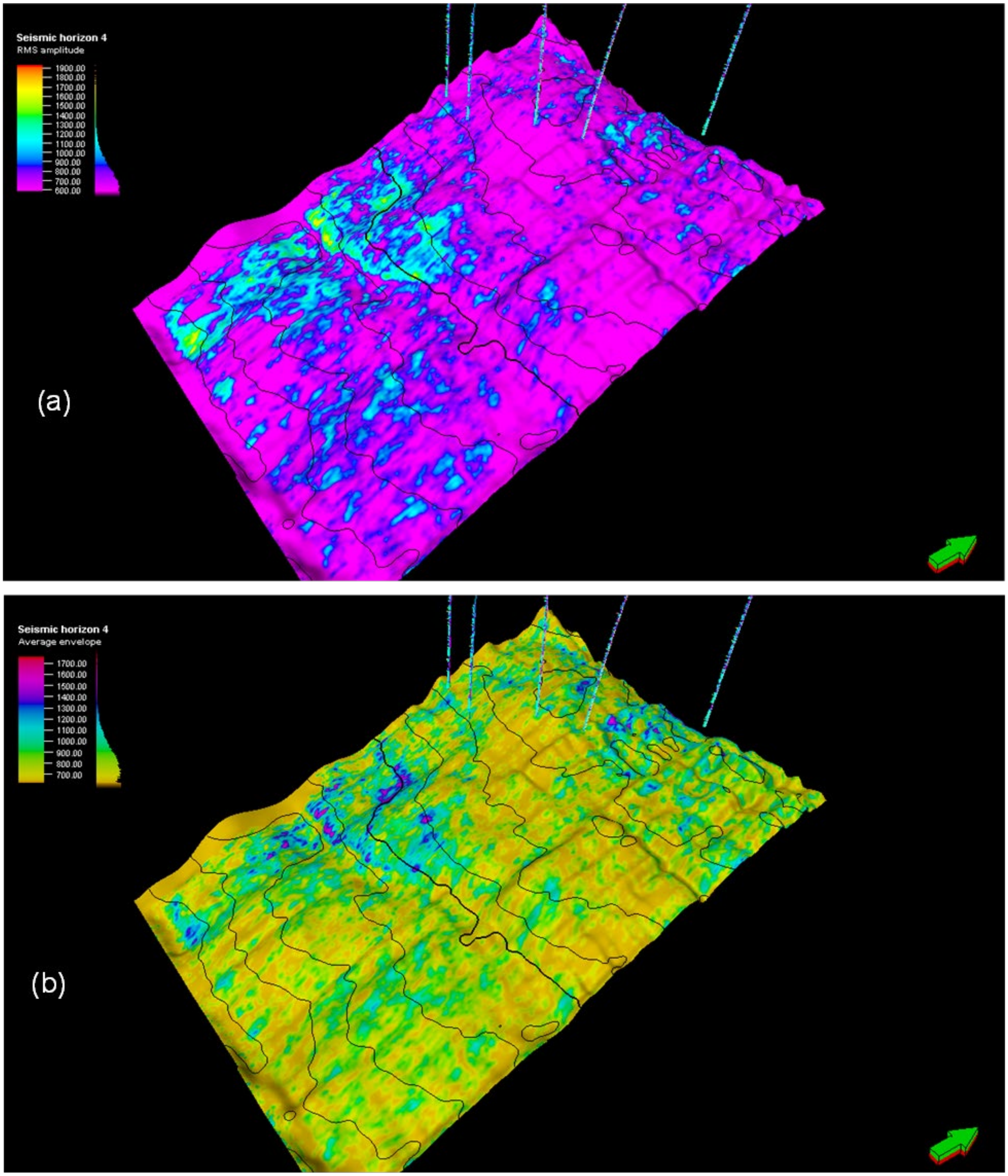

Fig. 11. 3D display of G_0006 reservoir top with the extracted (a) RMS amplitude and (b) Average Envelope attributes.

On the F_0004 reservoir top, regions of high RMS amplitude and Average Envelope observed in the northern part of the field clearly imaged hydrocarbon zones penetrated by the five wells evaluated in this study. However, some of the amplitude anomalies identified over G_0006 and H_0008 reservoir tops were not penetrated by the bit. Hence, the high anomalous zones identified in the western portions of G_0006 reservoir top and the three different anomalous zones on the H_0008 reservoir top are classified as hydrocarbon leads which may represent potential petroleum prospects at different stratigraphic intervals in the study area. In addition, high energy anomalies on reservoir intervals are a clear indication of hydrocarbon presence because energy is directly proportional to amplitude in fluids bearing formation, which has been identified on the surface attributes closing against the faults in the field. Amplitude is inversely proportional to the change in acoustic impedance, hence a zone bearing hydrocarbon usually has high amplitude and low impedance. From the anomalies, a zone of high amplitude value closing against a fault has been identified as undrilled hydrocarbon prospect in this study.

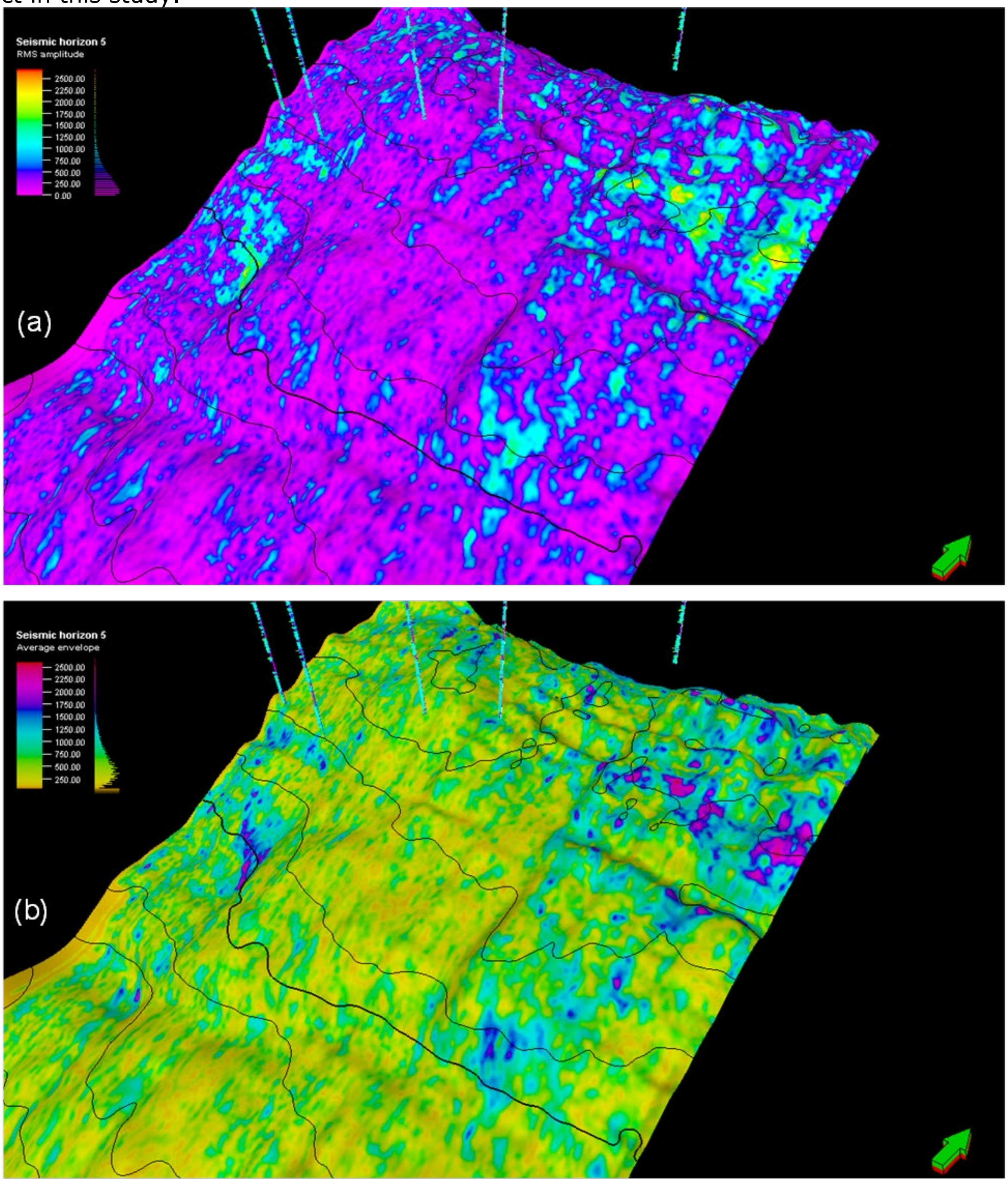

Fig. 12. 3D display of H_0008 reservoir top with the extracted (a) RMS Amplitude and (b) Average attributes.

The super-impositions of both RMS amplitude and Average Envelope attributes on depth top structural maps of the reservoir tops (Fig. 13, Fig. 14, and Fig. 15) showed zones of high amplitude within fault-dependent structural closures and stratigraphic traps. This validates the high amplitude supported closures as potential hydrocarbon prospects in the field.

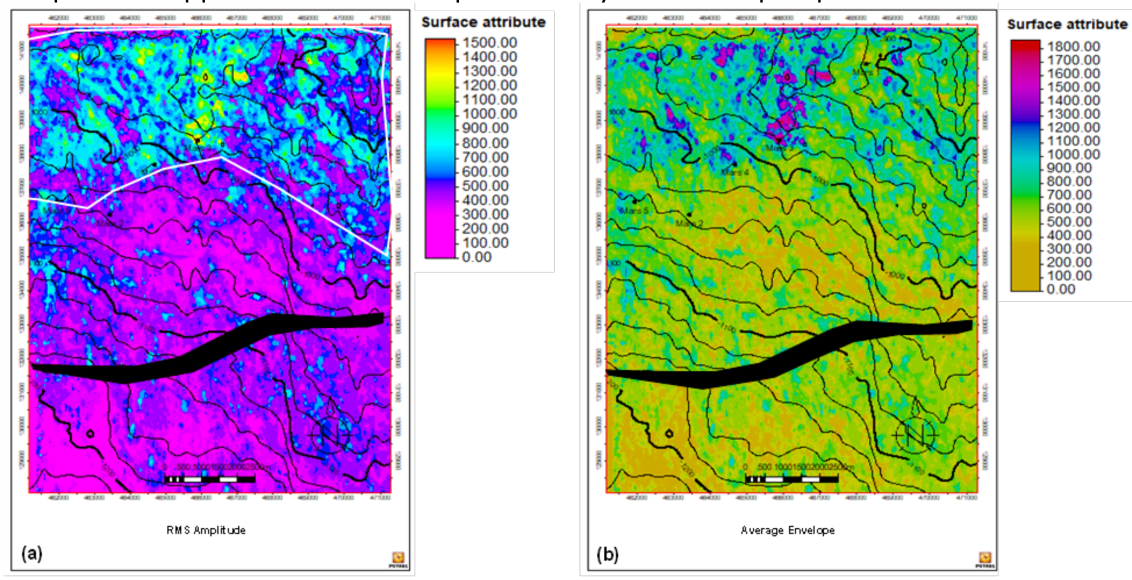

Fig. 13. Depth structure map of F_0004 reservoir top, with the extracted attributes (a) RMS Amplitude and (b) Average Envelope showing the delineated prospective zone (white polygon line).

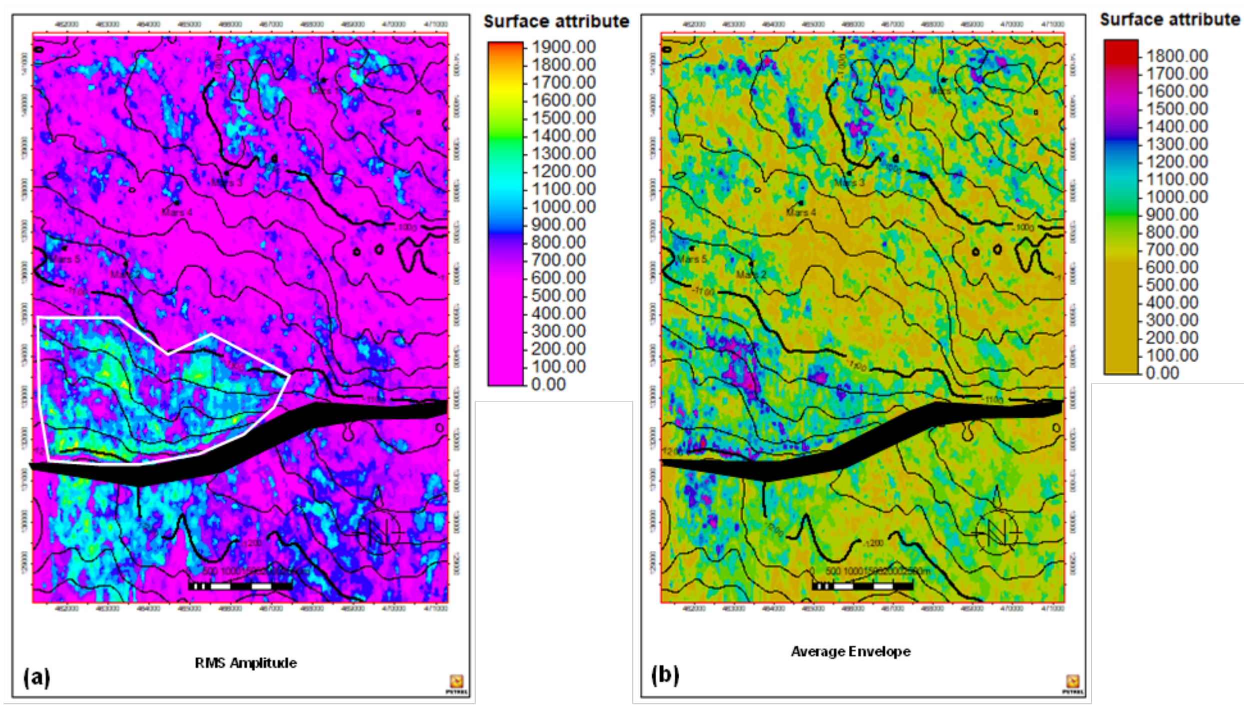

Fig. 14. Depth structure map of G_0006 reservoir top, with the extracted attributes (a) RMS Amplitude and (b) Average Envelope showing the delineated prospective zone.

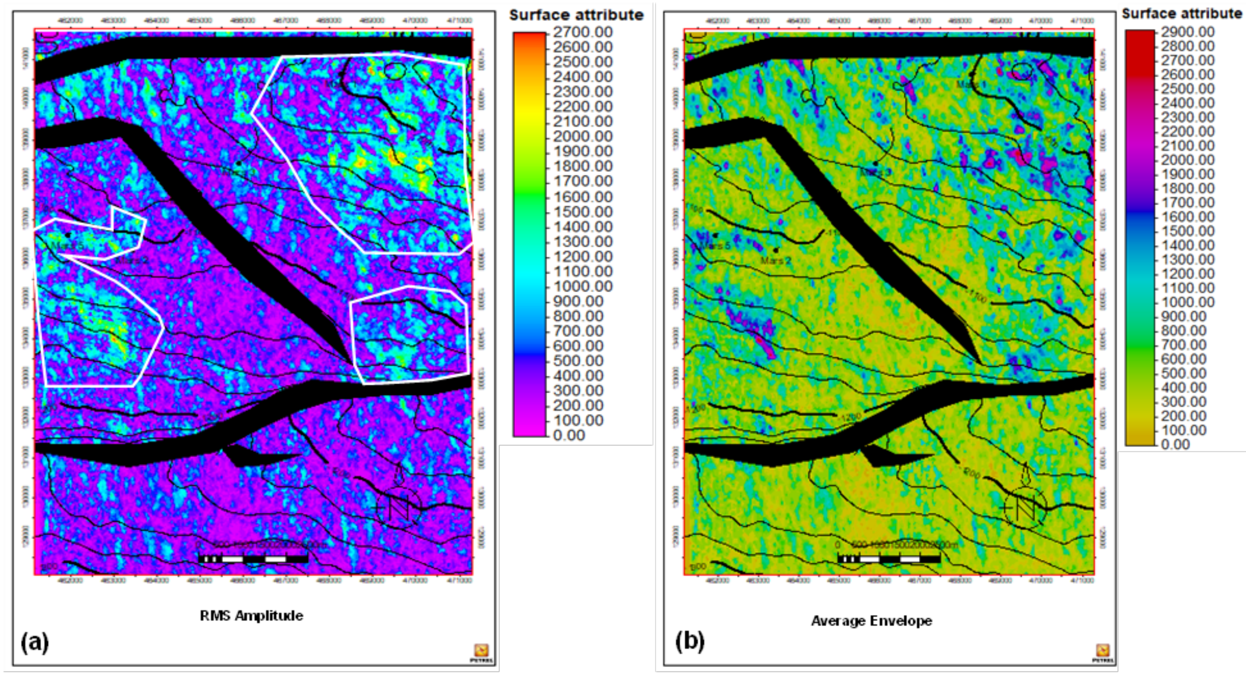

Fig. 15. Depth structure map of H_0008 reservoir top, with the extracted attributes (a) RMS Amplitude and (b) Average Envelope showing the delineated prospective zones.

The results from this study suggests a close relationship between hydrocarbon presence and strong amplitude anomalies on the extracted attribute maps. The attributes map of F_0004 reservoir top showed that the reservoir sand is possibly an anticlinal closure penetrated by the five producing wells in this study area. The presence of the producing wells suggests that the reservoir is charged with hydrocarbon. This closure is amplitude supported, with bright spot zones in the northern part of the field. The map revealed undrilled portions of the reservoir and thus, could be a useful guide to assess the overall reservoir performance, as well as in selecting infill-well locations for optimized drilling and hydrocarbon recovery.

The attributes map of G_0006 reservoir revealed amplitude-supported fault-dependent closures that has not been tested by the drill bits in the study area. The attributes map predicts hydrocarbon presence at the western part of this reservoir interval. Likewise, the attributes map of H_0008 reservoir showed three different amplitude-supported structural closures in the northeastern, eastern and western portions of this reservoir interval, that were not penetrated by the wells in the field. The closures are bounded by growth faults.

In general, the undrilled high amplitude portions of F_0004 reservoir and the identified high amplitude zones identified on G_0006 and H_0008 reservoirs are identified in this study as new hydrocarbon leads and prospect opportunities in the study area. However, further studies are required to ascertain the potentiality, producibility, and reservoir quality of the identified hydrocarbon zones in the field of study.

5. Conclusion

The integration of seismic attributes analysis and petrophysical evaluation using 3D seismic and well log data have aided the identification and delineation of potential hydrocarbon prospective zones in the "Mars" Field of the onshore Niger Delta Basin. The research which involved well log correlation and estimation of reservoir properties revealed three hydrocarbon-bearing reservoir sand units with good porosities and net-to-gross ratios, suggesting that they are high-quality sands. Detailed interpretation of the faults and horizons enabled better understanding of the structural framework which exerts a major control on the stratigraphy and trapping mechanisms in the study area. The identified trap styles include anticlinal closures and fault-dependent traps. The structural framework of the field increased in complexity with depth due to increase in gravity tectonics that created the growth faults.

Seismic attributes analysis was used to enhance the interpretation of structures (faults) and also played a key role in the identification of hydrocarbon leads that may be potential prospective zones in the field. RMS amplitude and Average Envelope attributes extracted on the interpreted reservoir tops revealed anomalously high amplitude zones interpreted to represent potential hydrocarbon leads/undrilled prospects in the field. These include high amplitude zones identified in the northern part of F_0004 reservoir top, the western portion of G_0006 reservoir top, and in the northeastern, eastern and western parts of H_0008 reservoir top. While some parts of the identified hydrocarbon leads/prospects on F_0004 reservoir top were penetrated by the five wells drilled in the field, the identified lead/prospects delineated both on G_0006 reservoir top and H_0008 reservoir top are yet to be tested by the bit. The high amplitude zones conformed with the structures mapped in the field. However, further studies integrating sequence stratigraphy, sedimentology, core data analysis, and reserves estimation are needed ascertain the hydrocarbon producibility of the field.

References

[1] Tuttle MLW, Charpentier RR, Brownfield ME. The Niger Delta Petroleum System: Niger Delta Province, Nigeria, Cameroon, and Equatorial Guinea, Africa. U. S. Geol. Surv. Open File Report. 99-50-H, 1999, p. 65.

[2] Dim CIP. Hydrocarbon Prospectivity in the Eastern Coastal Swamp Depo-Belt of the Niger Delta Basin – Stratigraphic Framework and Structural Styles. Springer Briefs in Earth Sciences. Springer International Publishing AG, Gewerbestrasse 2017, Switzerland, pp. 71.

[3] Ogbe OB, Orajaka IP, Osokpor J, Omeru T, Okunuwadje SE. Interaction between sea-level changes and depositional tectonics: implications for hydrocarbon prospectivity in the western coastal swamp depobelt, Niger Delta Basin, Nigeria. AAPG Bull., 2020; 104: 477–505.

[4] Ogbe OB, Okoro AU, Ogagarue, DO, Osokpor J, Overare B, Ocheli A, Opatola AO, Oluwajana OA. Reservoir hydrocarbon prospectivity and productivity evaluations of sands S-600 and S-700 of Fega field, onshore Niger Delta Basin, Nigeria. Journal of African Earth Sciences, 2021; 184: 1 – 12.

[5] Doust H, Omatsola E. Niger Delta. In J. D. Edwards, & P. A. Santogrossi (Eds.), Divergent and Passive Margin Basins. American Association of Petroleum Geologists, Memoir, 1990; 48: 201-238.

[6] Obimma KJ, Obiora DN, Oha AI, Ibuot JC, Yakubu JA. Seismic and Petrophysical Characterization of Reservoirs in Kjoe Field, Onshore Niger Delta, Nigeria. Pet Coal, 2021; 63(1): 50-62.

[7] Obiora DN, Gbenga D, Ogobiri G. Reservoir Characterization and Formation Evaluation of a “Royal Onshore Field”, Southern Niger Delta using Geophysical Well Log Data. Journal Geological Society of India, 2016; 87: 591-600.

[8] Falade A, Amigun J, Oyediran F. Seismic and Petrophysical Characterization of Subsurface Reservoirs within Arike Field, Niger Delta, Nigeria. Pet Coal, 2023; 65(2): 505-518.

[9] Madukwe CF, Anyiam OA, Okeugo CG, Dim CIP. Utilizing Seismic Attribute Analysis in Reservoir Evaluation and Hydrocarbon Prospectivity Studies in the “Zech” Field, Onshore Niger Delta Basin, Nigeria. Pet Coal, 2023; 65(3): 693-707.

[10] Reijers TJA. Stratigraphy and Sedimentology of the Niger Delta. Geologos, 2011;17(3): 133 - 162.

[11] Burke K, Dessauvagie TFJ, Whiteman AJ. Opening of the Gulf of Guinea and the geological history of the Benue depression and Niger delta. Nat. Phys. Sci. (Lond.) 1971; 233: 51–55.

[12] Murat R. Stratigraphy and paleogeography of the Cretaceous and Lower Tertiary in Southern Nigeria. African geology, 1972; 1(1): 251-266.

[13] Nwajide CS. Geology of Nigeria’s Sedimentary Basins. CSS Bookshops Ltd, Lagos, Nigeria, 2013, p. 565.

[14] Short KC, Stauble AJ. Outline geology of the Niger Delta. American Association of Petroleum Geologists Bulletin, 1967; 51: 761–779.

[15] Whiteman AJ. Nigeria: Its Petroleum Geology, Resources and Potential. Graham and Trotman, London, 1982, pp. 39.

[16] Larionov V. Radiometry of boreholes (in Russian). Nedra, Moscow, 1969; 127

[17] Asquith G, Gibson C. Basic well log analysis for geologists. Tulsa: American Association of Petroleum Geologists, 1982; 3.

[18] Chopra S, Marfurt KJ. Seismic attributes for prospect identification and reservoir characterization. Society of Exploration Geophysicists geophysical development series, 2007;11.

[19] Durrani MZA. "Quantitative seismic reservoir characterization of tight sands (granite wash) play at Stiles Ranch field in the Anadarko Basin, Texas(USA)." Proquest, ProQuest Dissertations and Theses; Thesis (Ph.D.) - The University of Tulsa, Dissertation Abstracts International, Volume: 76-12(E), Section: B., 2015, pp. 328

[20] Ojo BT, Olowokere MT, Oladapo MI. Quantitative Modelling of the Architecture and Connectivity Properties of Reservoirs in 'Royal' Field, Niger-Delta. Journal of Applied Geology and Geophysics, 2018; 6(2): 1-10.

[21] Asquith G, Krygowski D. Basic well log analysis (second edition). AAPG method in exploration series, No. 16, 2004, Tulsa.

[22] Evamy BD, Haremboure J, Kamerling P, Knaap WA, Molloy FA, Rowlands PH. Hydrocarbon habitat of Tertiary Niger delta. AAPG Bulletin, 1978; 62: 1-39.

[23] Gomes JS, Ribeiro MT, El Deeb M, Silva FP, Bockel-Rebelle RF. 'Lessons learned from Static Reservoir Modelling on Complex Carbonate Fields, Onshore UAE', SPE 88780, Presented at the 11th Abu Dhabi International Petroleum Exhibition and Conference held in in Abu Dhabi, U.A.E, 10-13 October, 2004.

To whom correspondence should be addressed: Eze Martins Okoro, Department of Geology, University of Nigeria Nsukka, Nigeria, E-mail: ezemartok@gmail.com ORCID: 0000-0002-8387-8489